

IDENTIFICATION AND CLASSIFICATION OF EARLY STAGE OVARIAN CANCER USING CONVOLUTIONAL NEURAL NETWORK

¹Ms. Kavitha S, ²Vidyaathulasiraman

¹Department of Computer Science, Periyar University, Salem

²Department of Computer Science Government Arts and Science College for Women, Bargur

Abstract. For old woman, ovarian cancer is a severe illness. Based on research, it is seventh major cause for woman death and fifth common disease worldwide. Using Artificial Neural Network (ANN), many researchers performed ovarian cancer classification. For making decision, doctors consider classification accuracy as an efficient factor. For giving proper treatment, doctors consider higher classification accuracy. Early and accurate diagnosis reduces mortality percentage and save lives. This paper proposes the novel annotated ovarian image classification using FR-CNN (fast region-based CNN) on the basis of ROI (region of interest) segmented. Here the input images have been classified into three types namely, epithelial, germ and stroma cells. This image has been preprocessed and segmented. After this annotation process takes places by using FR-CNN. The framework compares the manually annotated feature and trained feature in FRCNN for region based classification. This will help in analyzing the higher accuracy in detection of disease since manual annotation has lower accuracy in existing works so this work will experimentally prove that the machine learning based classification will yield higher accuracy. After the region-based training in FR-CNN, the classification is done by combining SVC-Support vector classifier and Gaussian Naives Bayes classifiers. Due to higher data indexing, the ensemble technique has been used in classification for the features. The simulation gives accurate part of input image to detect ovarian cancer.

Keywords: Ovarian cancer, annotated image classification, FR-CNN (Fast Region-based CNN), ROI (Region of Interest), SVM, Gaussian NB, Accuracy.

Received:

Accepted:

Published:

INTRODUCTION

In world, ovarian cancer is 2nd leading cancer which affects about 2% of female over their lifetime. If it is diagnosed in the earlier stage, it has 90% survival rate. Many research reports after investigation presents that early symptoms and indications of ovarian cancer are not clear [1]. For ovarian cancer, medical experts face several problems in producing cancer-screening guide-lines, there exists no single known cause or mark which leads to make it as silent killer. Research reports show that 90% of patients have symptoms long back before diagnosed [2]. Further, many patients experience numerous tumor metastasis, treatment cycles and disease recurrences. In female genital tract, while considering endometrial and cervical cancer, ovarian cancer is 3rd common cancer in Taiwan [3]. Figure 1 represents cervical, endometrial and ovarian cancer incidence rates in Taiwan from 1979 to 2013.

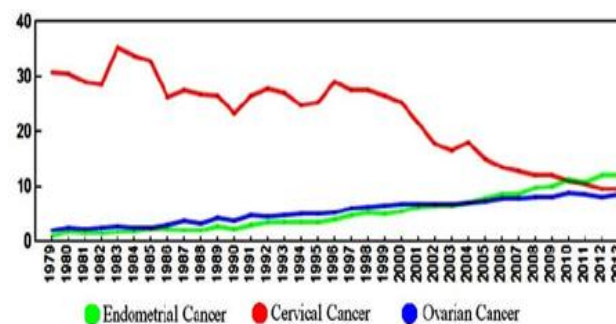


Figure 1: Incidence Rates

In 2013, there are 1321 cases in ovarian cancer, when compared with 162 cases in 1980 based on annual incidence rate data from Taiwan Cancer Registry. It was calculated that there

are 1500 new cases in 2014. Chances for Women survival with cancer are improved by early detection but it is tedious and no screening programs exists [4]. Literature insists that slow and late diagnosis maximizes mortality rates and recurrence rates. To predict ovarian cancer recurrence, there is enough data about signs, symptoms, protective factors and risks but no definite diagnostic tool exists at that time.

According to recent case studies related to control, women have many persistent or frequent non-specific symptoms. Symptoms are fullness or appetite loss, improved frequency or urinary urgency, abdominal or pelvic pain, weight loss, changes in bowel habit or fatigue. Based on the examination of general databases, women between 45 to 70 years old have a consultation with their general practitioner each year with any of the above symptoms, which means that these are common symptoms. For doctors, this gives diagnostic issue, low incidence ovarian cancer and in general every, 3-5 years, there is one woman with ovarian cancer by UK general practitioner and for diagnosis, low positive predictive values and lack of clear procedures. From the survey investigation of UK patients, 36% of women ovarian cancer diagnosis presents to physician with symptoms before diagnosis.

To improve diagnostic accuracy, reduce human resources and costs, in medical analysis machine learning was introduced. Machine learning (ML) is the field of Artificial Intelligence (AI) which is developed by using computer programs based on tasks and performance measures [5].

Significant characteristic of intelligent behavior is learning ability. Machine learning is a study of computational method to enhance performance on some tasks. Its aim may be technical, theoretical or cognitive. In technical analysis, for knowledge based systems knowledge acquisition process is automated. In theoretical analysis, learning method characteristics like limitations and scope are considered. It is inherently interdisciplinary area similar to AI. In the field of ML, statistic is widely used. Based on different methods such as knowledge representation, learning strategy and domain application, ML is classified. It consists for 4 major paradigms. They are neural networks, genetic algorithm and analytic, inductive and instance based learning. These all methods having same goal to enhance performance of few tasks which is done by determining and exploiting regularities in training data.

The issues are formulated into suitable ML methods by selecting, determining, gathering training data, estimating and fielding the learned knowledge. For learning process, training data forms basis. Learning technique only determines concepts in training data. In problem domain, selected instances and attributes have various situations. For applying ML method, training data construction is significant which has involvement of both domain expert and knowledge engineer. To describe training cases is significant task in determining learning data representation in which attributes are used. Hence larger attribute has more data than smaller one which is not required to produce good results. For quantitative ones by assigning consecutive numerical scores to ordinal category and nominal transferred to binary dummy attributes, ordinal attributes are used. Quantitative attributes are coded when learning needs discrete feature base. From large real-world dataset or set of instances from expert, training data is 'raw' sample which is extracted. Larger samples statistically provide reliable picture of task to be learned, but it is not optimum for the purpose of learning. Use of performance measure is objective way for calculating learning output. To characterize classifier performance, most measure called accuracy is used [6].

For further classification, training stage of ovarian cancer detection from same objects/patterns/class is grouped together and used as reference. In training stage, same features were extracted and compared with obtained references. Classification performance depends on the extracted features [7]. This paper aims to extract salient features and classify data whose results are used to develop a novel method cancer classification.

On knowledge basis, the symptoms of patients are classified to some particular group of disease by physicians. In this study, for ovarian disorders, learning classification model is learning task. By analyzing data, general classification method was learned. Using attribute

vectors (features or variables), training data containing cases like objects or instances are described. It may be quantitative or qualitative. Mutually exclusive cases and class information are used for learning in supervised learning. If all cases with identical attribute vector from same class, attributes are suitable for classification task.

Motivation

Cancer research is generally clinical and/or biological in nature, data driven statistical research has become a common complement. Predicting the outcome of a disease is one of the most interesting and challenging tasks where to develop data mining applications. Medical data mining is growing day by day and data are stored at rate of lakh in a second at a stretch. If incase to find a record or detail it is very hard to recollect the gynecological cancer database. To propose a model for early detection, prevent and correct diagnosis of the disease which will help the doctor in saving the life of the patient. The current research is being carried out on various ovarian cancer datasets using the data mining techniques to enhance the ovarian cancer prediction and diagnosis. The best prediction model has been identified which gives a high accuracy.

RESEARCH METHODOLOGY

The development in medical images provides more useful information hidden in image pixels where the medical practice/radiologists face difficulties to identify the power of diseases. Several approaches are being developed by the emerging researchers to solve this issue. The clinicians and radiologists show their interest in employing machine learning approaches particularly in detecting cancer. CAD methods are non-invasive but cost effective. Moreover, algorithms addressing heterogeneous medical image data are in demand. Hence, this research work attempts to employ machine learning approaches in detecting ovarian cancer. The architecture of this research methodology is illustrated in figure 2.

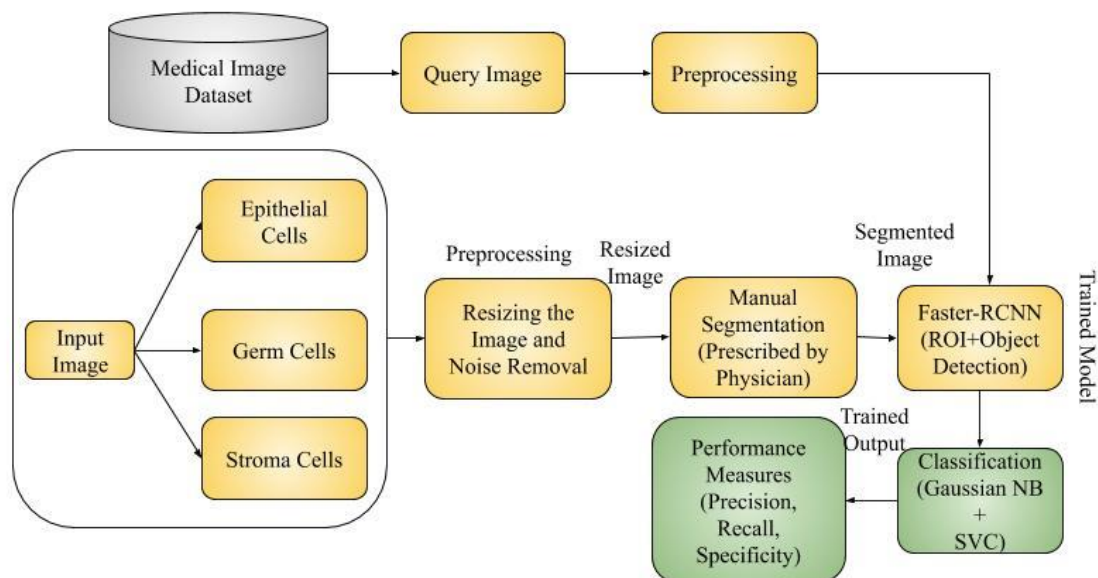


Figure 2: Architecture for proposed system

The input image has been classified into 3 types namely epithelial, germ and stroma cells. Initially the image is preprocessed for noise removal and filtering. This preprocessed image has been manually annotated and trained using normal training model. For compensation of manual annotation here this research is done using the neural network known as Fast Region Convolution Neural Network (FR-CNN). From the trained image and manually segmented image,

object is detection using FR-CNN. Here both features have been annotated based on region since the convolution is done for detecting edge. Contextual features have been annotated by image segmentation. The ratio of disease detection is lower manually and detection using computer aided diagnosis is higher in accuracy. Once FR-CNN is applied, Gaussian NB (Naives Bayes) and SVC (Support vector classifier) are used or classification.

Object Detection using FR-CNN

Fast Region CNN (FR-CNN) uses region proposal algorithm such as selective search to propose an estimated location of objects in an image. It is intuitive that the features extracted by CNN's are finally used to classify and give bounding boxes of the images. Thus, these extracted features have the information required to detect the objects in the image. FR-CNN architecture is built upon this observation. The region proposal algorithm (RPA) is replaced with region proposal network (RPN) that gives an estimate of regions with objects. This RPN is based on CNN and gives region proposal from the extracted features of CNN.

FR-CNN architecture thus is a combination of RPN which proposes regions and uses these proposed regions to give final bounding boxes of the object. Since both FR-CNN and RPN requires a CNN based feature extractor to perform almost similar task (in the end task of RPN is to give object regions only). A single feature extractor is used instead of using two separate models with the almost same weight. Figure3 shows the unified structure of FR-CNN and RPN. Anchor boxes are a major part of modern object detectors. In object detection, a rectangular box is obtained for each object in the image, thus there are multiple boxes of various shapes and sizes in each image.

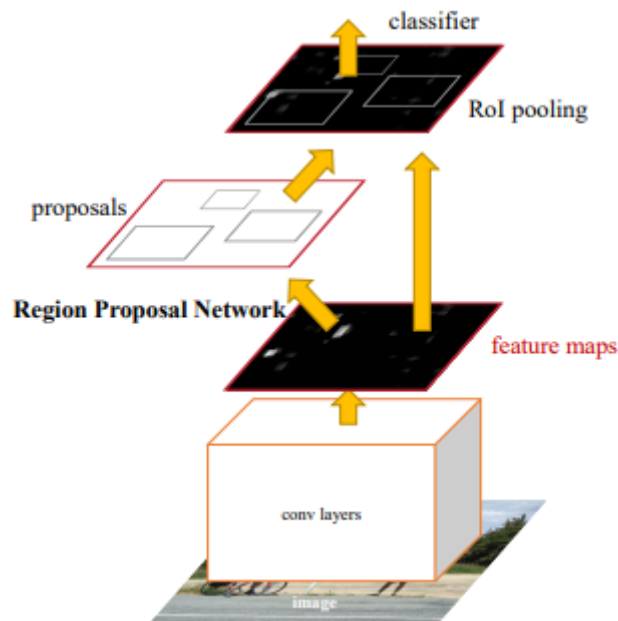


Figure 3: FR-CNN Network with RPN

First, the images are divided into grids. The reason is that medical images are usually pretty big. And you want to make sure to have labels (cancerous or non-cancerous) that are done by professionals for each grid. And each grid will be sent to the convolutional neural network to train. When sending each grid, a mask which belongs to the grid is also sent which says either “cancerous” or “non-cancerous”. Then, slide through each grid and make the neural network learn each grid with its mask. Only 3 anchor boxes of different aspect ratios are required). These anchor boxes are depicted in figure 4.

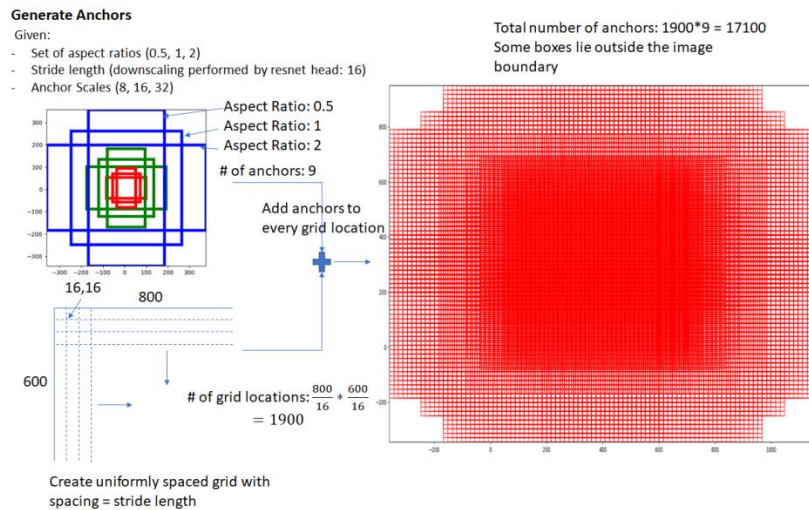


Figure 4: Anchor Boxes

k- Anchor boxes are generated for every pixel in the feature map (output of CNN). Thus the total number of anchor boxes is $h * w * k$ ($h * w$ is the output size of the feature map). K here is a hyper parameter. These k anchor boxes are of varying in sizes and aspect ratios which help covers objects of various shapes and sizes. The anchor boxes are hyperparameter specific to dataset and type of objects in that dataset (For example in some medical data if the object can be Instead of getting a raw regression output of an object, it is calculated as an offset to the anchor box. This offset in most cases will be a slight shift of the anchor box as these anchor boxes are placed all over the image. An object that is detected will be overlapped by multiple anchor boxes and not just 1. These redundant predictions are then later removed using non-max suppression. The output of our model is of $4 * k * h * w$ dimension (one box prediction for each anchor box, classification score is also predicted for each anchor box giving a probability of it containing object). This theoretically limits the number of objects that can be detected by CNN to $4 * k * h * w$, but in practice, this number is big enough. Anchor boxes can solve the issues of using multi scales at test time by using anchor boxes of various sizes (Red, Green, and Blue boxes in the above figure 4).

Region proposal network

Input of RPN is the feature map which produces a set of rectangular object proposals as output, each having an objectness score. The objectness measures score between object and background (thus low score for background and higher for regions with object). The region proposal time with selective search is 2 sec per image, whereas with RPN it's just 10ms.

FR-CNN uses anchor boxes of 3 aspect ratios and 3 scales. Thus, for each pixel in the feature map, there are 9 anchor boxes. The architecture is a simple convolution layer with kernel size $3 * 3$ followed by two fully connected (FC) layers (objectness score(classification) and regression of proposals). This fully connected layer is implemented using $1 * 1$ convolutional layers. The output size for the classification layer should be $2 * 9$ (foreground and background) and $4 * 9$ for the regression layer (Here 9 is a number of anchors for each pixel). The total number of predictions is now intuitive and will be $(4 + 2) * 9 * (H * W)$, for each pixel in feature map.

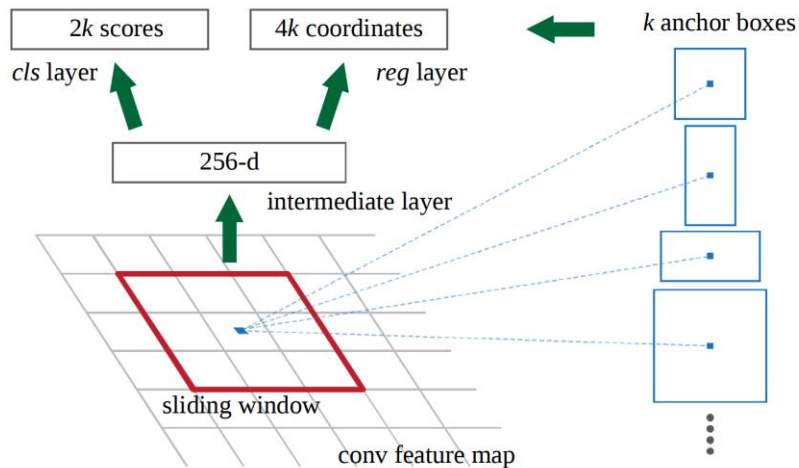


Figure.5: Faster RCNN

Loss Function

The loss function used in FR-CNN is

$$L(\{p_i\}, \{t_i\}) = \frac{1}{N_{cls}} \sum_i L_{cls}(p_i, p_i^*) + \lambda \frac{1}{L_{reg}} \sum_i p_i^* L_{reg}(p_i, p_i^*) \quad [1]$$

In this equation, p_i represents predicted probability (output from cls), and p_i^* is the ground truth similarly, t_i represents predicted bounding box and t_i^* stands for ground truth bounding box. L_{cls} are classification loss (log loss) and L_{reg} is smooth L_1 loss.

As discussed earlier regression offset is calculated from the nearest anchor box. To relate it with region proposal technique, anchor boxes are now acting as region proposal. For a feature map of size 40×60 , there are a total of $40 \times 60 \times 9 \sim 20000$ anchor boxes. All anchor boxes don't contribute to loss at the training time. The anchors with largest IOU with ground truth and anchor with IOU overlap larger than 0.7 are given positive labels. Anchors with IOU less than 0.3 are labeled as negative. Anchors that are neither positive nor negative has no contribution towards the training objective. Cross-boundary anchors are also ignored.

Training

FR-CNN architecture is a unified network with RPN and CNN layers are shared by both architectures. RPN and Fast RCNN cannot be trained separately (it will give different weights and thus CNN has to be passed twice for each of them). The authors used a 4-step training algorithm discussed below:

1. RPN trained initially and pre-trained weights from image-net are used.
2. FR-CNN is trained with proposals of step-1.
3. RPN is trained using convolution layers from step 2 and only layers unique to RPN are updated (weights of convolution layer is not updated).
4. Keeping this convolution layer, layers unique to Fast R-CNN are fine-tuned.

At training time, 20000 anchors(proposals) which are the output of RPN are first reduced by removing cross-boundary anchors (giving 6000 anchors). Non-max suppression (NMS) is applied to remove redundant predictions with a threshold of 0.7 (giving 2000 anchors). After NMS top-N ranked (classification score) proposal regions are used. For classification, Cross Entropy Loss with values 0 to 1 is used to measure the performance.

Smooth L1 loss for B-box regression is used, an absolute value between ground truth and prediction as L1 loss is less sensitive to outliers than loss like L2 which squares the error.

Testing

FR-CNN is a completely deep learning-based approach with a unified network and does not depend on algorithms like the selective search for proposals. Thus the image is directly passed to network giving predictions as output.

Every point in 37×50 is assumed as an anchor. Particular ratios and sizes are defined for every anchor (3 ratios and 3 sizes are 1:1, 1:2, 2:1 and 128^2 , 256^2 , 512^2 respectively for the actual image). RPN is connected with the convolutional layer containing 3×3 filters, 1 padding, and 512 output channels. Output is associated with two 1×1 convolutional layer for classification (determines whether box is an object or not) and box-regression as in figure 6.

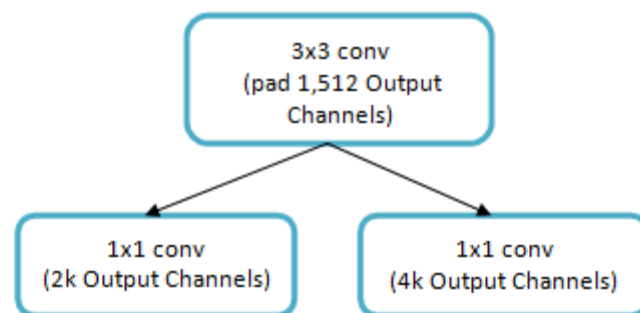


Figure 6: Convolutional implementation of an RPN architecture for k anchors

Here, each anchor has 9 boxes related to the actual image with the meaning that 16650 boxes exist in the actual image. But only 256 out of 16650 boxes are selected as a mini batch containing 128 foregrounds (positives) and 128 backgrounds (negatives). Simultaneously, non-maximum suppression is applied to avoid the overlapping of the proposed regions ROI. RPN ends after the processing the above steps. The next stage of FR-CNN is ROI pooling which is used for ROI whose output is $7 \times 7 \times 512$. This layer is then flattened with few FC layers. Finally, softmax function is applied for classification and linear regression for fixing the location of the boxes. The architecture of R-CNN is as in figure 7.

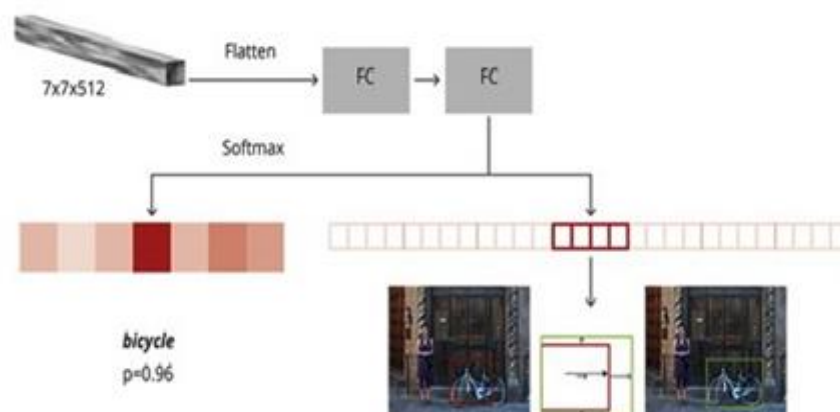


Figure 7: Architecture of R-CNN

Flow chart of Proposed FR-CNN system

Figure 8 illustrates the flow of the method introduced in this research work.

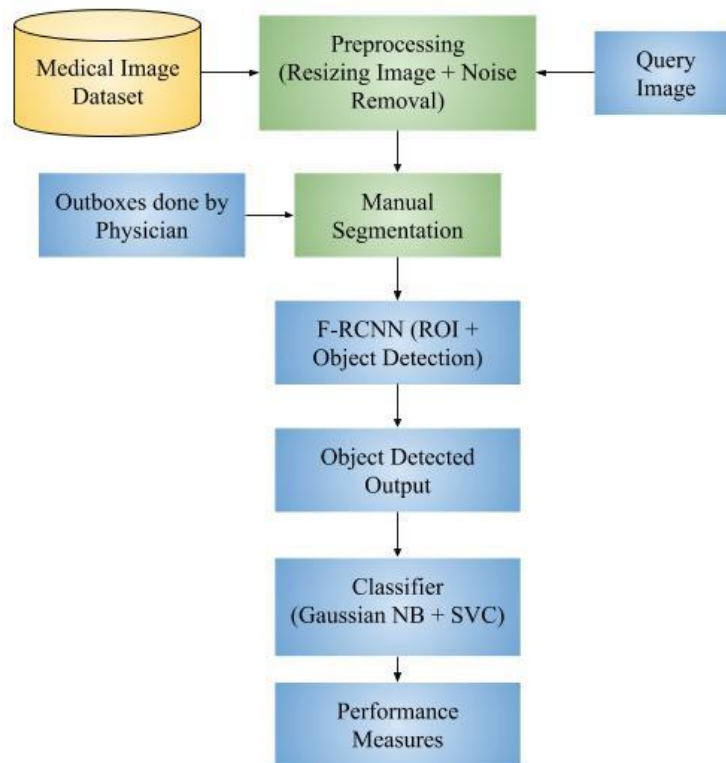


Figure 8: Overall flowchart for the proposed architecture

In algorithm 1 proposed ROI based segmentation with R-CNN classifier is presented.

Algorithm 1: ROI segmentation with R-CNN for Classification

Input: Input medical image database

Output: ROI based segmented R-CNN classifier

for every image in database do

Segmentation of color intensities of medical images img_{seg}

Estimate the boundaries of image with ROI estimation of boundaries and local pattern identification $lower_{ROI}$

Compute intersection of ROI region $lower_{ROI}$ and $upper_{ROI}$.

For upper ROI estimation compute upper image boundaries $upper_{ROI}$.

Perform segmentation of ROI intersected image $lower_{ROI}$ inset $upper_{ROI}$

Compute image feature extraction for ROI segmented image databases img_{seg}

end for

Generate classification model for CNN model with estimation of hyper parameters of medical



images CNN_{FE}

return img_{seg} and CNN_{FE}

Preparing training data and labels (get_anchor_gt)

Input is taken from the file called annotation.txt containing a several images with the information of bounding boxes. RPN method is used for creating these proposed boxes.

- Arguments taken

all_img_data: list(filepath, width, height, list(bboxes))

C: config

img_length_calc_function: calculates the size of feature map of the final layer based on the input imagesize

mode: 'train' or 'test'; augmentation is required for train mode

- Values Returned

x_img: resized and scaled image (least size is 300 pixels)

Y: [y_rpn_cls, y_rpn_regr]

img_data_aug: augmented actual image

debug_img: displays image for debugging

num_pos: displays the total positive anchors for debugging.

Calculation of RPN for every image (calc_rpn)

If the shape and anchor sizes of feature map are $18 \times 25 = 450$ and 9 respectively, then the potential anchors are $450 \times 9 = 4050$. Initially, the status of every anchor is 'negative'. Then, anchor is set to positive if IOU is more than 0.7. When IOU lies between 0.3 to 0.7, it is ambiguous and thus not considered in the objective. The drawback is that RPN holds several negative regions rather than positive, hence few negative regions are turned off. Total positive and negative regions are restricted to 256. `y_is_box_valid` checks whether anchor has an object. `y_rpn_overlap` finds out whether this anchor and ground-truth bounding box overlaps.

Both `y_is_box_valid` and `y_rpn_overlap` are 1, If anchor is positive.

Both `y_is_box_valid` and `y_rpn_overlap` are 0, if anchor is neutral.

`y_is_box_valid` is 1 and `y_rpn_overlap` = 0 for negative anchor.

- Arguments taken

C: config

img_data: augmented image data

width: width of actual image

height: height of actual image

resized_width: resized width based on C.im_size

resized_height: resized height based on C.im_size

img_length_calc_function:

- Values Returned

y_rpn_cls: list(num_bboxes, `y_is_box_valid` + `y_rpn_overlap`)

y_is_box_valid: returns either 0 or 1 (0 represents that box is invalid and 1 represents a valid box)

y_rpn_overlap: returns either 0 or 1 (0 represents that the box is not an object while 1 represents that the box is an object)

y_rpn_regr: list(num_bboxes, $4 * y_rpn_overlap + y_rpn_regr$)

y_rpn_regr: x_1, y_1, x_2, y_2 coordinates of bunding boxes

`y_rpn_cls` has (1, 18, 25, 18) as shape and the size of feature map is 18×25 . Every point of the feature map has 9 anchors where every anchor holds 2 values

for `y_is_box_valid` and `y_rpn_overlap` respectively. Hence $9 \times 2 = 18$ is the 4th shape.

y_rpn_regr is (1, 18, 25, 72) as shape and the size of feature map is 18x25. Every point of the feature map has 9 anchors where every anchor holds 4 values for tx, ty, tw and th respectively. These 4 values have their own y_is_box_valid and y_rpn_overlap. Hence, $9 \times 4 \times 2 = 72$ is the 4th shape.

Calculation of ROI from RPN (rpn_to_roi)

- Arguments taken (num_anchors = 9)

rpn_layer: output layer for rpn classification

shape (1, feature_map.height, feature_map.width, num_anchors)

is (1, 18, 25, 9)

regr_layer: output layer for rpn regression

shape (1, feature_map.height, feature_map.width, num_anchors*4)

is (1, 18, 25, 36)

C: config

use_regr: checks if bboxes regression can be used in rpn

max_boxes: maximum number of bboxes for NMS

overlap_thresh: When iou > threshold in NMS, drop box

- Values Returned

result: boxes from NMS (shape is 300, 4)

boxes: bboxes' coordinates

From the above step, for 4050 anchors, max_boxes have to be extracted as ROI and has to be passed to the classifier layer. In the function, at first, boxes overstepping original image are deleted. Then, NMS with the threshold value of 0.7 is used.

RoIPooling layer and Classifier layer (RoIPoolingConv, classifier layer):

RoIPooling layer processes ROI with a specific size with the use max pooling. Every ROI is partitioned as few sub-cells, and max pooling is applied to every sub-cell. The shape of the output is the number of sub-cells. Classifier layer, final layer lying behind RoIPooling layer is used for predicting the class name for every input anchor and regression of bounding box.

- Arguments taken

base_layers: vgg

input_rois: `(1,num_rois,4)` list of rois, with ordering (x,y,w,h)

num_rois: ROIs to be processed at a time (it is 4 here)

- Values Returned

list(out_class, out_regr)

out_class: output of the classifier layer

out_regr: output of the regression layer

Initially, flatten the pooling layer followed with two FC layer and 0.5 dropout. At last, outputs two layers.

out_class: softmax activation function which classifies class name of the object

out_regr: linear activation function for coordinates of boxes regression

- The ROI pooling layer, special type of spatial pyramid pooling (SPP) layer, has a single pyramid level which primarily partitions the features from selected proposal windows that are the outcomes of region proposal algorithm into sub-windows with size h/H by w/W . Pooling operation is performed on every sub-window which produces output as fixed-size features (H x W) regardless of input size. The values chosen for H and W are 7 such that the output suits well with first fully-connected layer. ROI pooling is performed on each channel individually.

- ROI Pooling layer produces the output as $N \times 7 \times 7 \times 512$ where N is the total proposals which are provided as inputs for the successive fully connected layers, softmax and BB-regression branches. Softmax classification branch gives probability values of every ROI with K categories and one catch-all background category. The output of BB regression makes the bounding boxes from RPA more accurate.

Loss:

The softmax layer classification provides the probabilities for each ROI over $(K + 1)$ categories $p = p_0, \dots, p_K$. Classification loss $L_{loc}(p, u)$ is given by $-\log(p_u)$ which is the log loss for the true class u . Smooth L1 loss for BB regression is given by,

$$L_{loc}(t^u, v) = \sum_{i \in \{x, y, w, h\}} \text{smooth}_{L_1}(t_i^u - v_i) \quad [2]$$

Regression gives 4 bounding box offsets t_i^k where $i = x, y, w$, and h . (x, y) represents top-left corner while w and h are width and height of the bounding box. The true bounding box regression aiming at class u is given as v_i when $u \geq 1$. When $u=0$, it is ignored since background classes have no ground truth boxes. Smooth L loss is given by equation 1 and multi-task loss of every ROI is the integration of two losses given by equation 2. FR-CNN having an integrated learning scheme, fine-tunes backbone CNN and performs classification and regression of bounding box.

Training

- At the training stage, every mini-batch is created from $N=2$ images. Mini-batch has 64 ROIs for every image.
- Similar to RCNN, 25% of the ROIs are object proposals with $\text{IoU} > 0.5$ with a ground-truth bounding box of a foreground class which is positive and labeled with appropriate $u=1 \dots K$.
- The rest of ROIs are sampled from proposals having IoU with ground truth bounding boxes between $[0.1, 0.5)$ are labelled as background class $u = 0$.
- Prior to the ROI pooling layer, the whole image passes through CNN. Hence, every ROI of the same image share memory and computation in both forward as well as backward passes through CNN.
- The sampling of every ROI of very few images goes through feature generation, classification, and regression modules. But, in SPP Nets, almost all ROIs of different images goes through training process to detect only fine tunes the fully connected layers after the feature generation as it is infeasible for updating weights before the SPP layer. Few ROI's have huge receptive fields on the actual image. The original features still are extracted from a pre-trained network which was trained for classification that restricts the accuracy of SPP Nets.
- The network's batch size is too small for CNN until the batch size of ROI pooling layer is 2, but larger for softmax and regression layers with batch size 128.
- **Back propagation through ROI pooling layer:** For every mini-batch ROI r , consider ROI pooling output unit y_{rj} as max-pooling output of sub-window $R(r, j)$. After then, gradient is accumulated in the input unit (x_i) in $R(r, j)$ when position i is the argmax chosen for y_{rj} as in figure 9.

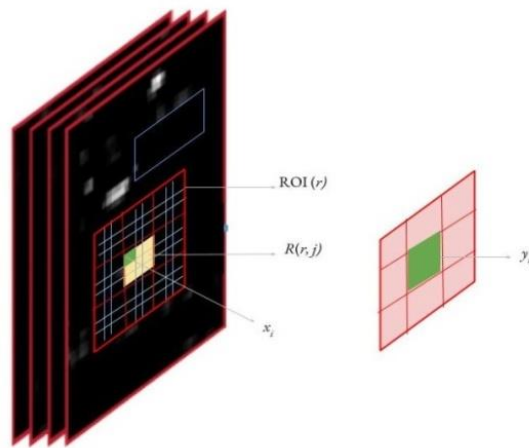


Figure 9: Back propagation through ROI pooling layer

- In FR-CNN multi-scale pipeline, inputs are resized as randomly sampled size during training such that it is scale invariance. During testing, every image is given to the network with multiple fixed scales. For every ROI, features are pooled from any one of these chosen scales such that the pixels of scaled candidate window are closer to 224 x 224. But, single scale pipeline performs better with less computing time cost. In the single-scale method, every image during training and testing are resized to 600 with upper cap of 1000.
- Larger fully connected layers are compressed using truncated SVD approach such that network is more effective. Then, a layer parameterized by W , weight matrix, is factorized to minimize parameter count by dividing it as two layers (ΣV^T and U with biases) with no non-linearity between these layers, where $W \sim U \Sigma V^T$.

SVC (Support Vector Classifier)

SVCs, a kind of large-margin classifier, are a set of supervised learning approaches which learn the dataset utilized for both classification and regression. Moreover, the aim of SVC vector space-based machine learning approach is to discover **decision boundary** between two classes which is far from any point in the training data. SVC classifies by generating an abstraction of vectors named as support vectors which is a part of training vector set. Data can be separated as training and testing set to achieve better classification. In training set, for every occurrence, there exists a target value and several features. SVC is employed as it provides a model based on training data. Using the features of the test data, target values are forecasted. SVCs primary objective is to classify tasks but it has been extended to learning tasks and regression. SVC, generally a binary classifier, produces either positive or negative output of the learning function. The linear boundary of the data is used to classify patterns between two classes. Support Vectors are the co-ordinates of individual observation. Kernel approach is employed in SVC for non-linear classification which converts low dimensional input space to higher ones. Moreover, non-separable classes are converted as separable ones based on data labels.

When SV points are far from hyperplane, the probability of classifying the points correctly is also more in their corresponding region. SV points critically determine hyperplane as the change in the position of vectors alters the position of the hyperplane. This hyperplane is technically known as *margin maximizing hyperplane*.

This algorithm aims in finding a hyper plane with N -dimensions where the data points are classified such that the margin is maximized. N dimension varies as per the number of features. Comparison of two features is carried out smoothly. However, when numerous features are classified, it is not straight forward always. When the margins are maximized, more accurate prediction is obtained.

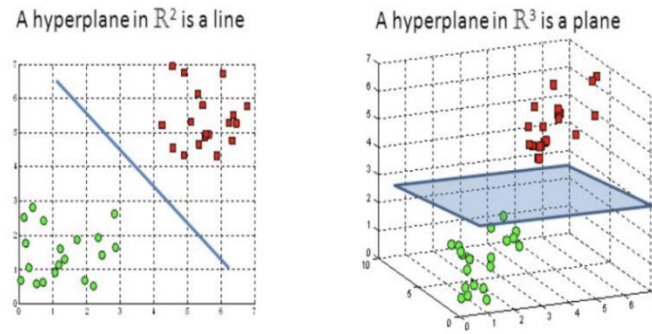


Figure 10: Support vector visualization

Gaussian NB (Naives Bayes)

Naïve Bayes is a fast and straightforward approach used for classification which works on the basis of Bayes theorem and is represented as:

$$P(X|Y) = \frac{P(Y|X)P(X)}{P(Y)} \quad [3]$$

This classifier considers that every variable equally contributes to the outcome independently. At this point, every feature is independent to each other and output is also affected with same weight. Hence, Naïve Bayes theorem cannot be applied to the issues related to real-life and only low accuracy is obtained when this algorithm is used. Hence, Gaussian NB, a kind of NB, is used which considers that the features adopt normal distribution. The possibility of features is assumed to be Gaussian and has a conditional probability. Gaussian NB is given below:

$$P(x_i|y) = \frac{1}{\sqrt{2\pi\sigma^2}} \exp\left(\frac{-(x_i - \mu_y)^2}{2\sigma^2}\right) \quad [4]$$

RESULTS

This section discusses about the performance analysis for the proposed technique in ovarian cancer detection which is compared with the existing methods. Confusion matrix shows the model performance based on true negatives, true positives, and false negative and false positive

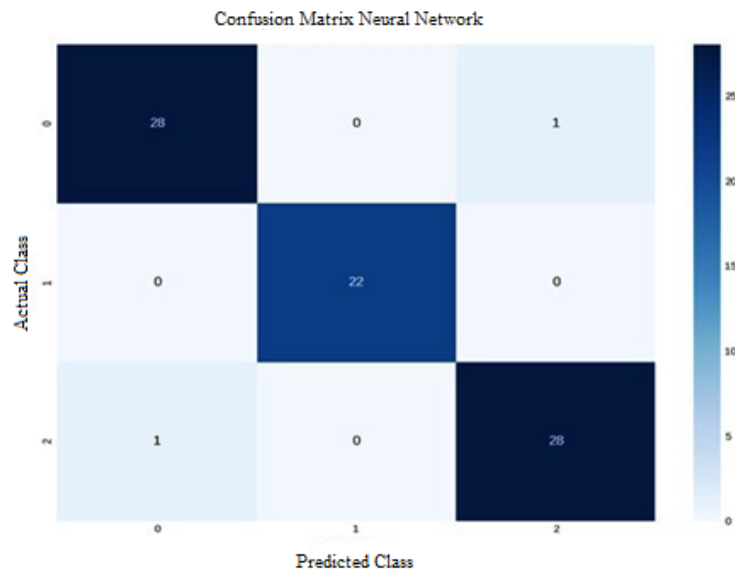


Figure11.Confusion matrix of Gaussian NB using FR-CNN

The above figure 11 shows the confusion matrix of Gaussian NB using FR-CNN in which the rows represent the predicted class (output class) and columns denotes the actual class (target class) of data pertaining to ovarian cancer. The diagonal blue and white cells denote the trained network that is correctly and incorrectly classified. The column on the right side indicates every predicted class while the row at bottom represents the performance of every actual class. This confusion matrix plot for Gaussian NB using FR-CNN shows that the overall classification attains 98.69% correct classification performance.

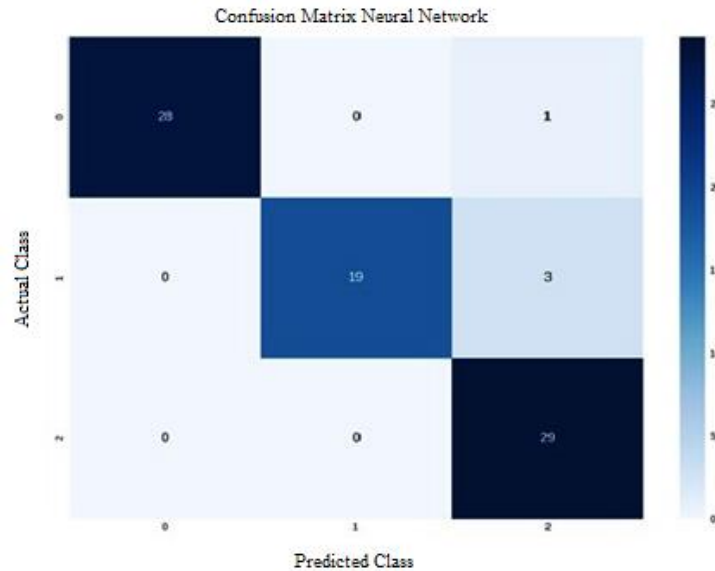


Figure12.Confusion matrix of SVC using FR-CNN

The above figure 12 shows confusion matrix of SVC using FR-CNN with rows and columns indicates predicted and actual classes respectively. This confusion matrix plot for SVC using FR-CNN shows that all overall classification achieves 97.39%. The column on the right side indicates predicted class while the row at bottom represents the performance of every actual class. Here, zeroes are hidden in order to easily analyze the performance. From this confusion matrix, more often few couples are recognized wrongly. Table 1 shows the analysis of SVC and Gaussian NB with various parameters.

Table 1 .Analysis of SVC and Gaussian NB Classifiers

Parameters	SVC (%)	Gaussian NB (%)
Precision	95.96	97.7
Recall/Sensitivity	94.31	97.7
Specificity	97.39	98.69

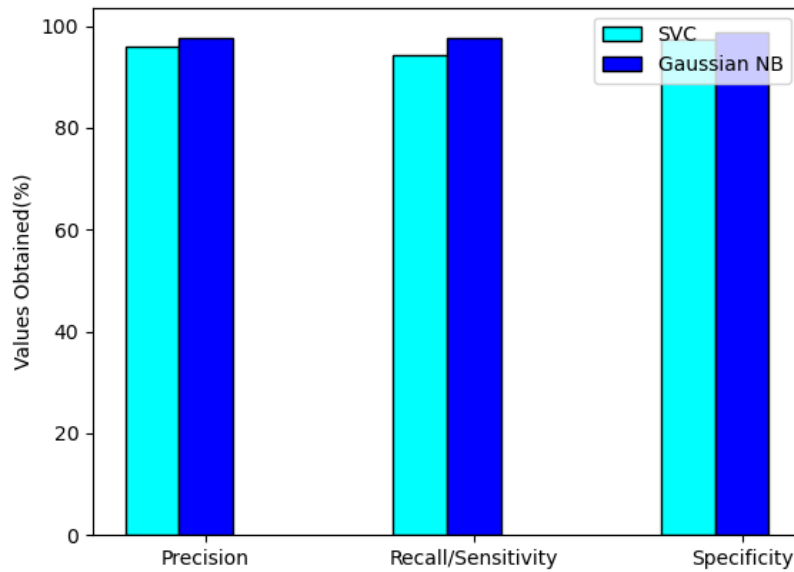


Figure13. Classification graph of Gaussian NB and SVM using FR-CNN

The above figure 13 shows the graphical representation based on the parameters for Gaussian NB and SVM using FR-CNN. The parameters taken are precision, Recall/sensitivity and specificity has been calculated in %. In precision value of SVC gives 95.96%, and Gaussian NB gives 97.7% where precision is enhanced in Gaussian NB using FR-CNN. For recall/sensitivity it gives 94.31% for SVC and 97.7% using Gaussian NB and also for specificity SVC value is 97.39% and 98.69% for Gaussian NB using FR-CNN. From this above discussion, the Gaussian NB technique in classification using FR-CNN gives enhanced predicted class in ovarian cancer detection. Table 2 compares the parametric values obtained for various methods.

Table2: Comparative Analysis of various parameters for various methods

Parameters	KNN (%)	CNN (%)	DCNN (%)	SVC (%)	Gaussian NB (%)
Precision	78.45	81.91	89.19	95.96	97.7
Recall/Sensitivity	74.19	79.02	88.28	94.31	97.7
Specificity	95.33	82.93	91.91	97.39	98.69

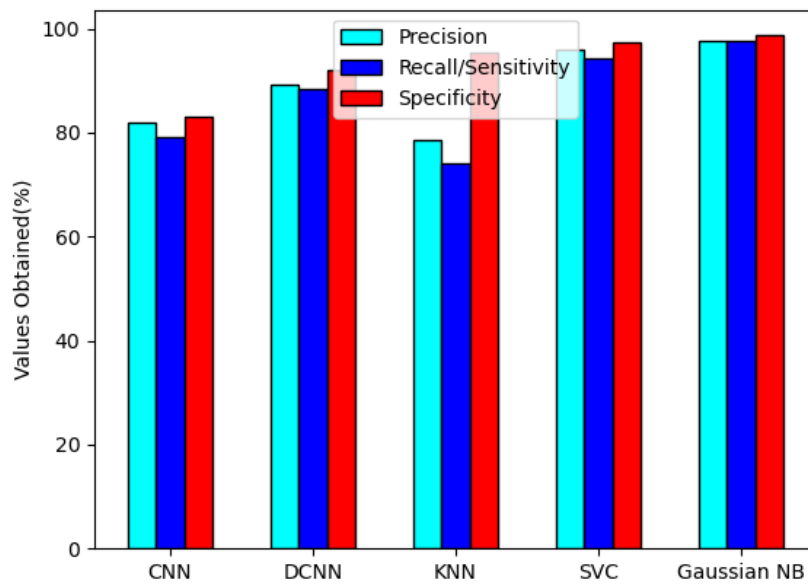


Figure14: Overall comparison between proposed and existing algorithms

The above graph shows overall comparison for precision, recall, specificity for existing and proposed techniques. For precision, CNN gives 81.91%, DCNN gives 89.19%, KNN gives 78.45%, SVC gives 95.96% and Gaussian NB gives 97.7% among these techniques SVM and Gaussian NB gives optimum value. For recall, CNN is 79.02%, DCNN is 88.28%, KNN gives 74.19%, SVS gives 94.31%, and Gaussian NB gives 97.7%. For specificity, CNN gives 82.93%, DCNN gives 91.91%, KNN gives 75.33%, and SVC gives 97.39% and Gaussian NB 98.69%. Among all the techniques proposed SVC and Gaussian NB using FR-CNN has obtained enhanced value.

CONCLUSIONS

Hence from the performance analysis, it shows that the classification technique of both SVC and Gaussian NB using FR-CNN gives the precision value more than 95% when compared with existing techniques. Among this classification technique 97% to nearly 99% of precision has obtained from the predicted class using this proposed FR-CNN. Based on the performance of the proposed model, it is concluded that this ovarian cancer detection classification model is a vital contribution in the medical field which helps the physicians to take the precise decision and treat the patients in a better way. However, no public ovarian cancer dataset was considered for classification in this research. Hence, it can be focuses to use ovarian cancer dataset for classification as the future enhancement of this research work.

REFERENCES

- Chen K, Niu Y, Wang S, Fu Z, Lin H, Lu J and Xia D, "Identification of a Novel Prognostic Classification Model in Epithelial Ovarian Cancer by Cluster Analysis", *Cancer Management and Research*, vol.12, 2020.
- Liu Z, Wu H, Deng J, Wang H, Wang Z, Yang A and Tang X, "Molecular classification and immunologic characteristics of immunoreactive high-grade serous ovarian cancer", *Journal of cellular and molecular medicine*, vol.24, no.14, pp.8103-8114, 2020.
- Arfiani A and Rustam Z, "Ovarian cancer data classification using bagging and random forest", *AIP Conference Proceedings*, vol. 2168, no.1, 2019.

- Shafi, Uroosa and Sugandha Sharma, "Ovarian Cancer Detection in MRI Images using Feature Space and Classification Method", *International Journal of Recent Technology and Engineering (IJRTE)*, vol.8, no.2, 2019.
- Mangone L, Mandato VD, Gandolfi R, Tromellini C, Abrate M, "The impact of epithelial ovarian cancer diagnosis on women's life: a qualitative study", *European Journal of Gynaecol Oncol*, vol.35, no.1, pp.32-8, 2014.
- BHP, "Health Survey by the Bureau of Health Promotion BHP)", <https://cris.hpa.gov.tw/pagepub/Home.aspx>, 2017.
- Nolen BM and Lokshin AE, "Screening for ovarian cancer: old tools, new lessons", *Cancer Biomark*, vol.8, no.4, pp.177-86, 2010.
- Liang C and Peng L, "An automated diagnosis system of liver disease using artificial immune and genetic algorithms", *Journal of medical systems*, vol.37, no.2, pp.1-10, 2013.
- Jelovac D and Armstrong DK, "Recent progress in the diagnosis and treatment of ovarian cancer", *CA Cancer Journal of Clin*, vol.61, no.3, pp.183-203, 2011.
- Karbalay-Doust S and Noorafshan A, "Stereological estimation of ovarian oocyte volume, surface area and number: application on mice treated with nandrolonedecanoate", *Folia Histochem. Cytobiol*, vol.50, pp.275-279, 2012.
- İnik and Özkan, "A new method for automatic counting of ovarian follicles on whole slide histological images based on convolutional neural network", *Computers in biology and medicine*, vol.112, 2019.
- Massimo Mazzini and Franco Giorgi, "The follicle cell-oocyte interaction in ovarian follicles of the stick insect *Bacillus rossius* (Rossi): (Insecta: Phasmatodea)", *Journal of Morphology*, vol.185, no.1, pp.37-49, 2016.
- González-Reyes A and St Johnston D, "Patterning of the follicle cell epithelium along the anterior-posterior axis during *Drosophila* oogenesis", *Development*, vol.125, no.15, pp.2837-2846, 1998.
- Drosophila* oogenesis, "The Wellcome/CRC Institute and Department of Genetics", *University of Cambridge*, pp.2837-2846, 2018.
- Carole L. Browne and William Werner, "Intercellular junctions between the follicle cells and oocytes of *Xenopus laevis*", *Journal of Experimental Zoology*, vol.230, no.1, pp.105-113, 2014.
- Wu and Miao, "Automatic classification of ovarian cancer types from cytological images using deep convolutional neural networks," *Bioscience reports*, vol.38, no.3, 2018.
- Vasavi G and Jyothi S, "Classification and detection of ovarian cysts in ultrasound images", *International Conference on Trends in Electronics and Informatics (ICEI)*, pp.783-787, 2017.
- Schorge J. O, Modesitt S. C, Coleman R. L, Cohn D. E, Kauff N. D, Duska L. R and Herzog T. J, "SGO White Paper on ovarian cancer: etiology, screening and surveillance", *Gynecologic oncology*, vol.119, no.1, pp.7-17, 2010.
- Hiremath P. S and Jyothi R. Tegnoor, "Automated ovarian classification in digital ultrasound images", *International Journal of Biomedical Engineering and Technology*, vol.11, no.1, pp.46-65, 2013.
- Nawgaje, Devesh D and Rajendra D. Kanphade, "Hardware Implementation of Genetic Algorithm for Ovarian Cancer Image Segmentation", *Proceedings of the International Journal of Soft Computing and Engineering (IJSCE)*, vol.2, no.6, pp.304-306, 2012.